Chapter 2
BDS/GNSS Real-Time Kinematic Precise Point Positioning with Un-differenced Ambiguity Resolution

Lizhong Qu, Qile Zhao, Jing Guo, Guangxing Wang, Xiangxin Guo, Qiang Zhang, Kecai Jiang and Liang Luo

Abstract BeiDou Navigation Satellite System (BDS) is constructed and operated by China independently. It has important significance in researching the real-time kinematic precise point positioning (PPP-RTK) based on BDS. The fusion of multi-GNSS in data processing can increase satellites observed, improve the geometric configuration of satellites constellation, enhance the accuracy, continuity and reliability in real-time kinematic positioning. This paper deduced the mathematical model of BDS/GNSS PPP-RTK, studied the theories and methods of BDS/GNSS un-difference ambiguity resolution, and realized multi-GNSS PPP-RTK by fixing the un-differenced ambiguities of BDS-only, GPS-only, both BDS and GPS satellites, respectively. Multi-GNSS data of reference stations from Crustal Monitor of Network of China (CMONOC) were processed. The experiment results showed that the values of fractional cycle bias (FCB) of BDS IGSO and MEO satellites kept stable; The precision were less than 1 cm in plane direction and 3 cm in vertical direction after the fusion of BDS, GPS and GLONASS even without ambiguity resolution, respectively; It not only raised the precision of positioning but also quicken the convergence speed after fixing the un-differenced ambiguities of BDS IGSO and MEO satellites; The performance of multi-GNSS PPP-RTK improved further after fixing the un-differenced ambiguities of both BDS and GPS satellites.

Keywords BDS · GNSS · Real-time kinematic precise point positioning · Un-differenced ambiguity resolution · Fractional cycle bias

L. Qu (✉) · Q. Zhao · J. Guo · G. Wang · X. Guo · Q. Zhang · K. Jiang · L. Luo
GNSS Research Center, Wuhan University, 129 Luoyu Road, Wuhan 430079, China
e-mail: qulizhong@whu.edu.cn

J. Sun et al. (eds.), *China Satellite Navigation Conference (CSNC) 2015 Proceedings: Volume III*, Lecture Notes in Electrical Engineering 342,
DOI 10.1007/978-3-662-46632-2_2

2.1 Introduction

Beidou Navigation Satellite System (BDS) is constructed and operated by China independently, which is the third mature Global Navigation Satellite System (GNSS) by following the US GPS and the Russian GLONASS. From December 27, 2012 on, BDS began to provide regional service officially. Nowadays, BDS satellite constellation is composed of 5 GEO, 5 MEO and 4 IGSO satellites [1]. Domestic and foreign scholars have carried out a large number of studies on the precise orbit determination and precise positioning of BDS [2–6]. The accuracy of BDS satellites' orbit radial direction reached 10 cm by using Wuhan University PANDA software package [5, 6]. The fusion of multi-GNSS data effectively increase the number of satellites observed, improve satellite spatial geometry construction. Thus, the integration of multi-GNSS data can improve the positioning accuracy, continuity and reliability [7–10].

Traditional precise point positioning using un-differenced and ionosphere-free pseudo-range and phase combination measurements can obtain positioning results of centimetre level. But the fractional bias of the hardware delay result in the loss of integrity character of un-differenced integer ambiguity and the float solutions are acquired [11]. Currently, the un-differenced ambiguity resolution researches focused on the GPS system. There were three main methods: decoupled clock model, single-difference between satellites model and integer phase clock model [12–16]. By ignoring the effect of receiver and satellite terminal pseudo-range hardware delay on phase ambiguity, Geng et al. proved the equivalence of single-difference between-satellites model and integer phase clock model [17]. Without any assumption, Shi et al. proved the three methods equivalent by deducing the rigorous formulas and comparing computational efficiency of the three methods [18]. BDS adopt Code Division Multiple Access (CDMA) signal, which is the same as GPS. So the GPS ambiguity resolution methods were able to be used on BDS. Based on the single-difference between satellites ambiguity resolution method, we realized GNSS real-time PPP by fixing the BDS-only, GPS-only and combined BDS/GPS ambiguity. As we all known, the signal establishment system of GLONASS is Frequency Division Multiple Access (FDMA). The hardware delay in receiver terminal between satellites cannot be eliminated directly by using single-difference between satellites. As a result, the ambiguity resolution of GLONASS satellites is more complicated [19]. In this manuscript, we just consider the ambiguity resolution of BDS and GPS satellites.

2.2 Data Collection

24 stations with Multi-GNSS data from Crustal Monitor of Network of China (CMONOC) were chosen as reference stations in this paper. The stations distribution is shown in Fig. 2.1. All stations just contain GPS, BDS and GLONASS observations. Figure 2.2 shows the sky plots of GPS, BDS and GLONASS satellites tracked at WUHN station. As we can see that, the distribution of GPS satellites tracked is

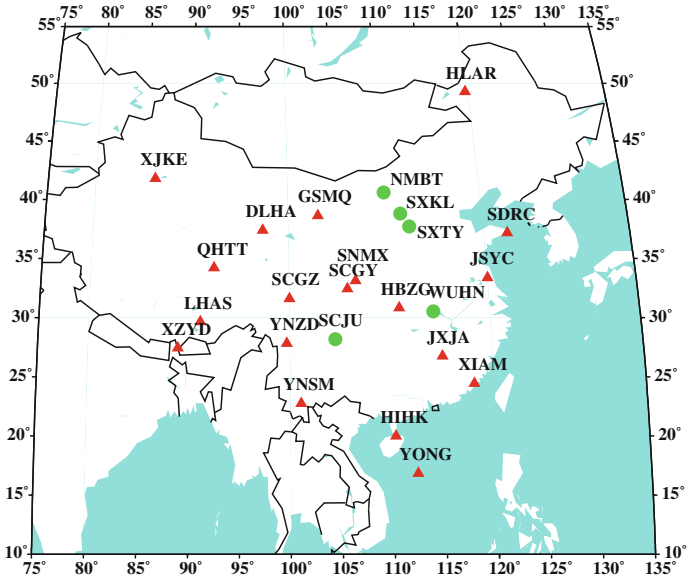

Fig. 2.1 CMONOC GNSS stations distribution for FCB estimation and ambiguity resolution

more balanced than that of GLONASS and BDS and the satellites distribution after the integration of multi-GNSS is more intensive. Figure 2.3 shows the time series of DOP values and number of satellites tracked at WUHN station. The integration of multi-GNSS improved the geometric configuration of satellite constellation, increased the number of observable satellites, which can improve the accuracy, enhance the continuity and the reliability in navigation and positioning service.

2.3 Processing Strategy

2.3.1 Mathematical Model

Precise point positioning mathematical model based on original dual-frequency ionosphere-free combination is:

$$P_r^s = \rho_0^s + c(dt_r - dt^s) + m_r^s T_r + c(B_r - B^s) + e_s \tag{2.1}$$

$$L^s = \rho_0^s + c(dt_r - dt^s) - \lambda n^s + m_r^s T_r + c(b_r - b^s) + \varepsilon_s \tag{2.2}$$

where ρ_0^s is the geometric distance between station r and satellite s. dt_r is the receiver clock error. T_r is the residual error of wet troposphere delay. m_r^s is the mapping function of wet troposphere delay. n^s is integer ambiguity. B_r, b_r are receiver terminal hardware delay of pseudo-range and phase, respectively. B^s, b^s are satellite terminal

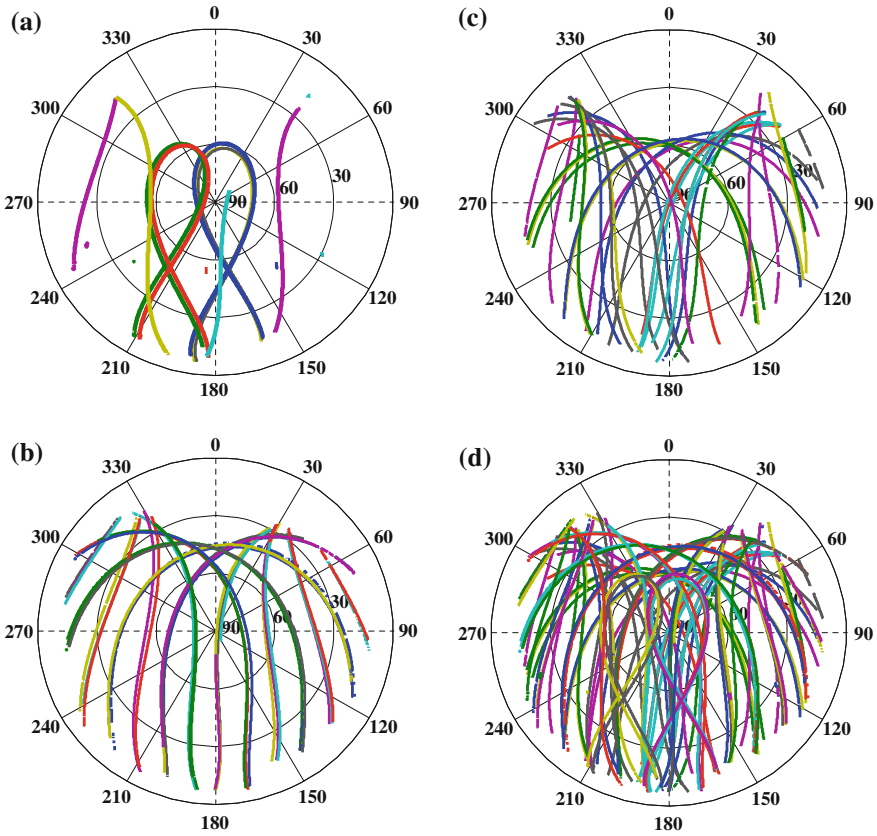

Fig. 2.2 Sky Plot of BDS, GPS and GLONASS at WUHN. **a** BDS. **b** GLONASS. **c** GPS. **d** BDS/GPS/GLONASS

hardware delay of pseudo-range and phase, respectively. e_s, ε_s are measurement noise of pseudo-range and phase, respectively, which includes the multipath errors. During parameter estimation, pseudo-range hardware delay B_r is absorbed by the receiver clock error. Formulas 2.1 and 2.2 are usually written as:

$$P^s = \rho_0^s + c \cdot \delta t_r + m_r^s T_r + e_s \tag{2.3}$$

$$L^s = \rho_0^s + c \cdot \delta t_r - \lambda n^s + m_r^s T_r + \varepsilon_s \tag{2.4}$$

where,

$$\delta t_r = dt_r + B_r \tag{2.5}$$

$$N^s = n^s + c(b_r - b^s - B_r + B^s)/\lambda \tag{2.6}$$

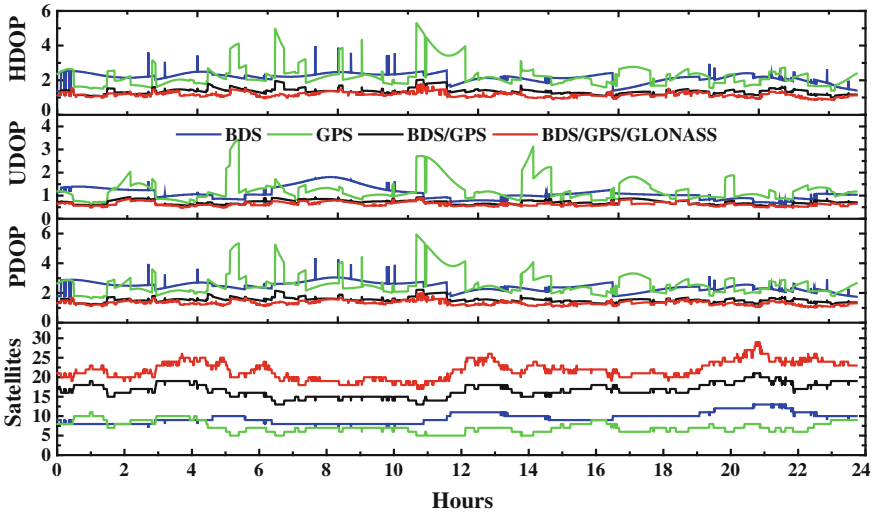

Fig. 2.3 Time series of DOP and satellites tracked at WUHN

Multi-GNSS PPP mathematical model is written as:

$$\begin{cases} P^G = \rho_0^G + c \cdot \delta t_r^G + m_r^G T_r + e_G \\ L^G = \rho_0^G + c \cdot \delta t_r^G - \lambda^G N^G + m_r^G T_r + \varepsilon_G \\ P^B = \rho_0^B + c \cdot \delta t_r^G + c\delta t_r^{B-G} + m_r^B T_r + e_B \\ L^B = \rho_0^B + c \cdot \delta t_r^G + c\delta t_r^{B-G} - \lambda^B N^B + m_r^B T_r + \varepsilon_B \\ P^R = \rho_0^R + c \cdot \delta t_r^G + c\delta t_r^{R-G} + m_r^R T_r + e_R \\ L^R = \rho_0^R + c \cdot \delta t_r^G + c_r^{R-G} - \lambda^R N^R + m_r^R T_r + \varepsilon_R \end{cases} \tag{2.7}$$

where,

$$\delta t_r^{B-G} = \delta t_r^B - \delta t_r^G \tag{2.8}$$

$$\delta t_r^{R-G} = \delta t_r^R - \delta t_r^G \tag{2.9}$$

Compared with GPS and BDS, the signal structure of GLONASS is FDMA, which results in internal frequency bias (IFB) between satellites. In this paper, the IFBs were not estimated that were absorbed into the pseudo-range residual and phase ambiguity.

2.3.2 Ambiguity Resolution Process

Real-time un-differenced ambiguity resolution contains two steps: (a) estimate the satellite FCB of wide-lane and narrow-lane; (b) ambiguity resolution at rovers.

2.3.2.1 FCB Estimation

As Formula 2.6 shown, the initial phase and hardware delay are strongly correlated with the ambiguity. After merging the hardware delay of the phase and code in the receiver terminal with those in the satellite terminal, Formula 2.6 can be written as:

$$N^s = \tilde{N}^s + \beta_r - \beta^s \tag{2.10}$$

The integer part of the hardware delay in the receiver and satellite terminal are difficult to separate from the ambiguity and the fractional cycle bias (FCB) of them broke the integer character of ambiguity. We can use the classic LAMBDA method to fix the ambiguity as long as FCBs were separated accurately from the integer part. The process to calculate the wide-lane and narrow-lane FCB is shown as follows:

(1) Firstly, we solve the real wide-lane ambiguity based the Melbourne-Wübbena (MW) combination observation and then separate the integer part N^s_{mw} of the ambiguity from the FCB $(\beta_r - \beta^s)_{mw}$ by rounding directly;
(2) Secondly, we construct the single-difference between satellites by using wide-lane FCB $(\hat{B}_r - \hat{B}^j)_{mw}$ to eliminate the FCB in receiver terminal. Then, all the same satellite pair FCBs of all the stations are acquired to calculate the average values. Assuming that n satellites were tracked by all the stations in the same time, we could get $n(n-1)/2$ average FCB values. After that, we use the least-square adjust with the quasi-stable datum or gravity datum method to get the wide-lane and narrow-lane FCB of every satellite;
(3) Thirdly, the GPS daily static station coordinates by using PANDA software package are regard as the "ground truth" and the precise orbit and satellite clock error are used to calculate the un-differenced real ambiguity. The fixed wide-lane ambiguities are subtracted from the real ambiguity to get the real narrow-lane ambiguities. Then, we can get the satellite narrow-lane FCB by following Steps (1) and (2).

2.3.2.2 Ambiguity Resolution at Rovers

The satellite wide-lane and narrow-lane FCBs of the reference network are broadcasted to rovers in real-time. Firstly, we separate the wide-lane FCBs from the wide-lane observations to fix the wide-lane ambiguities in a short initial time. Meanwhile, we acquire the real solutions of un-differenced ambiguities and the real solutions of the narrow-lane ambiguities can be solved out by using Formula 2.11. Then, the satellites narrow-lane FCBs are subtracted from the real solutions of narrow-lane ambiguities. After separating the receiver narrow-lane FCBs, the classic LAMBDA method is used to search and fix the narrow-lane ambiguities.

Finally, the fixed ambiguities are used to update the positions and we can get the integer solutions [20].

$$N_{nl}^{s} = \frac{f_1 + f_2}{f_1} N^{s} - \frac{f_2}{f_1 - f_2} N_{wl}^{s} \tag{2.11}$$

where, N_{nl}^{s} is the real un-differenced ambiguity, N_{wl}^{s} is the integer un-differenced wide-lane ambiguity.

2.3.3 Data Processing Strategy

Precise orbit and clock corrections are BDS/GPS/GLS/GALIEO multi-GNSS products generated by Wuhan University PANDA software package [6]. The sampling interval of precise satellite clock corrections is 30 s. The prior standard deviation of PC and LC observations of BDS, GPS and GLONASS satellites are 0.2 and 0.002 m, respectively. During the parameter estimation, GPS and GLONASS satellites antenna PCO and PCV are corrected and BDS satellites antenna PCO are corrected for BDS satellites PCV are unknown. The PCO and PCV of receiver antenna are unknown. Meanwhile, the troposphere delay, the phase winding and the tidal effect are considered. The cutoff elevation angle is 7°. The specific observation model is shown in Table 2.1.

2.4 Results Analysis

Data on September 27, 2014, were processed in this paper (day of year is 260) and the sample interval is 30 s. 19 stations were taken as reference stations, which were the red triangle in Fig. 2.1. The wide-lane and narrow-lane FCB of BDS MEO and IGSO satellites and GPS satellites were estimated and provided to the rovers. When constitute single difference observations between satellites, we selected one satellite from the same system as the reference star. The FCB initialization time was 1200 s and the FCBs were upgraded every 30 s. In addition, 5 stations were taken as rovers to compare the accuracy of PPP-RTK float and fixed solutions, which were the green cycles in Fig. 2.1. We processed the static data to simulate the kinematic condition in BDS-only, GPS-only, combined BDS/GPS and combined BDS/GPS/GLONASS mode. But only the ambiguities of BDS and GPS were fixed. The GPS daily static solutions by using PANDA software package were taken as the “ground truth” for the 5 rovers. By comparing the float and fixed solutions with the “ground truth”, we analyzed the convergence time and the accuracy after convergence in the East, North and Up components for each mode.

Table 2.1 BDS/GNSS PPP-RTK measurement model and parameters estimation strategy

Observation model	
Observables	Un-differenced Ionosphere-free combination (PC and LC)
Elevation mask	7°
Interval	30 s
Precise orbit	PANDA software precise orbit: BDS/GPS/GLONASS/GALIEO [6]
Precise satellite clock error	PANDA software 30 s precise satellite clock correction: BDS/GPS/GLONASS/GALIEO
Satellite antenna PCO	GPS, GLS: IGS08.atx, BDS Default
Satellite antenna PCV	GPS, GLS: IGS08.atx, BDS unknown
Phase wrapping	Considered [21]
Receiver antenna PCO and PCV	Unknown
Tropospheric	Hydrostatics and wet-component delay: Saatamoien model, mapping function: VMF1
Ionosphere	Eliminate first order ionosphere by using PC and LC observations
Solid tide, ocean tide, pole motion	IERS conventions 2010
Parameter estimation	
Estimator	Square root information filter [22]
Base station coordinate (for estimating FCB)	GPS Daily Static Solution by using PANDA software, 3D Accuracy 1 cm
Wide-lane and narrow-lane FCB upgrade interval	30 s
FCB initial time	1200 s for both GPS and BDS satellites
Rovers coordinate (PPP)	Random-walking, 5 m, 10 cm $\sqrt{\Delta t}$
Receiver clock error	White noise
Tropospheric	Piece-wise-constant, 2 h interval
System time in receiver terminal	White noise
Integer ambiguity	Estimated as constant. Fix all GPS satellites, fix all BDS IGSO and MEO satellites

2.4.1 FCB Stability Analysis

Figure 2.4 shows the time series of the un-differenced wide-lane and narrow-lane FCBs of GPS satellites. Figure 2.5 shows the time series of the un-differenced wide-lane and narrow-lane FCBs of BDS IGSO and MEO satellites. In the two figures, the upper panel is the wide-lane FCB time series and the lower panel is the narrow-lane FCB time series. As we can see, the un-differenced wide-lane and narrow-lane FCB of GPS satellites are relatively stable in time domain and only a few satellites fluctuate in the initial stage. The changes of all the satellites keep within 0.2 cycles. The un-differenced wide-lane and narrow-lane FCB of BDS MEO satellites are also

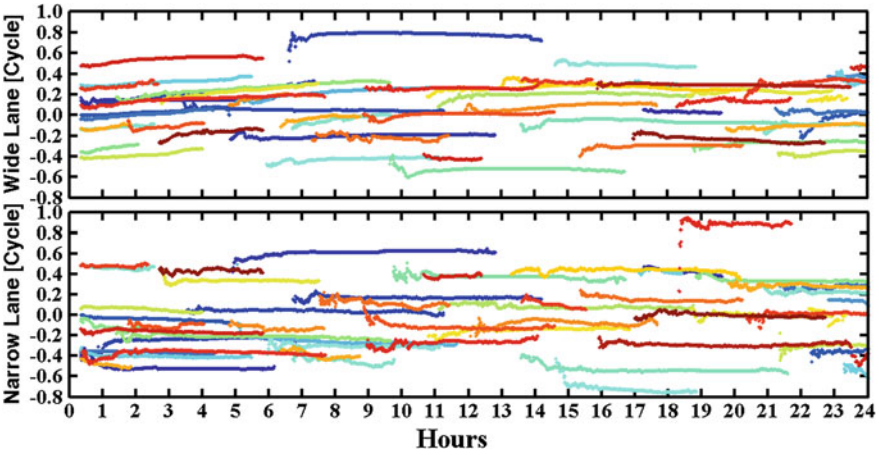

Fig. 2.4 Time series of GPS satellites wide-lane and narrow-lane FCB of CMONOC

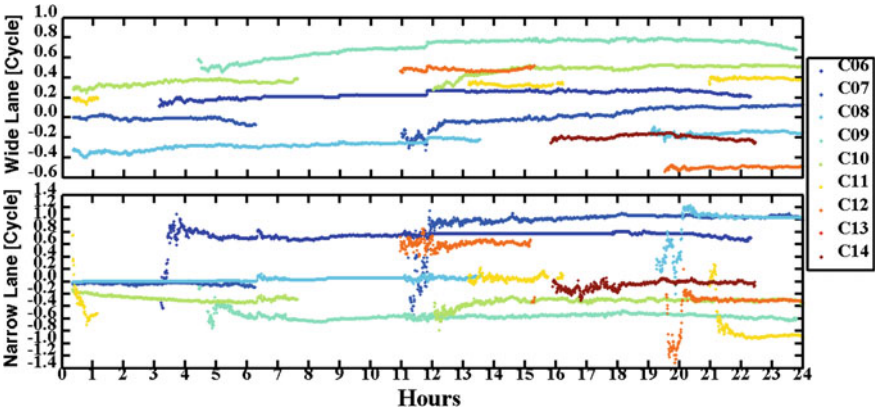

Fig. 2.5 Time Series of BDS IGSO and MEO satellites wide-lane and narrow-lane FCB of CMONOC

relatively stable in time domain and the changes keep within 0.2 cycles, while the wide-lane FCB of BDS IGSO satellites seem less stable than those of GPS satellites and BDS MEO satellites, the changes of the IGSO satellites reach 0.2–0.4 cycles. The narrow-lane FCB of BDS IGSO and MEO satellites are relatively stable after convergence while fluctuate larger than those of GPS satellites in the initial stage. As Formula 2.11 shown, the convergence time of the narrow-lane ambiguities depend on the wide-lane and un-differenced ambiguities. The length of FCB initial time seems enough for GPS and BDS wide-lane FCB estimation. But as Figs. 2.7 and 2.8 shows, BDS PPP needs more convergence time than that of GPS. During the convergence stage, the narrow-lane FCB change with the un-differenced ambiguity.

2.4.2 Positioning Results

Figure 2.6 shows the differences of BDS-only, GPS-only, BDS/GPS and BDS/GPS/GLONASS PPP float and fixed solutions against the "ground truth" in East, North and Up components. Table 2.2 shows the average values of RMS of the differences of BDS-only, GPS-only, BDS/GPS and BDS/GPS/GLONASS PPP of the rovers. We can find that:

(1) The RMS of the differences of BDS PPP float solutions for all the rovers are better than 5, 2 and 7 cm in East, North and Up components, respectively. The average values of the RMS are 2.8, 1.9 and 5.9 cm, respectively. The RMS of GPS PPP float solutions are better than 3, 2 and 4 cm, respectively. The average values are 2.2, 1.2 and 3.2 cm, respectively. The East and North components of BDS PPP float solutions are very close to those of GPS PPP while the Up component is far from that of GPS, which mainly dues to the worse orbit accuracy of BDS. Compared with BDS-only and GPS-only PPP, the accuracy of combined BDS/GPS positioning has improved significantly. The RMSs are better than 2, 1 and 3 cm, respectively. And the average values are 1.3, 0.7 and 2.6 cm, respectively. The accuracy improved 40.9, 41.7,

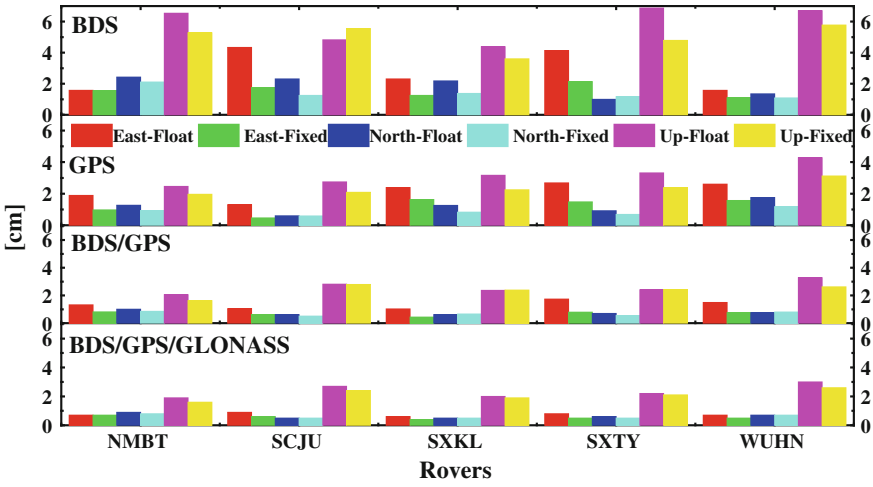

Fig. 2.6 RMS of float and fixed solutions of BDS, GPS, BDS/GPS and BDS/GPS/GLONASS PPP

Table 2.2 Average values of RMS of float and fixed solutions of BDS, GPS, BDS/GPS and BDS/GPS/GLONASS PPP

RMS	East (cm)		North (cm)		Up (cm)	
System	Float	Fixed	Float	Fixed	Float	Fixed
BDS	2.8	1.6	1.9	1.4	5.9	5.0
GPS	2.2	1.2	1.2	0.8	3.2	2.4
BDS/GPS	1.3	0.7	0.7	0.7	2.6	2.4
BDS/GPS/GLONASS	0.7	0.5	0.6	0.5	2.3	2.1

18.8 % and 53.6, 63.2, 55.9 % than that of GPS-only and BDS-only PPP. The RMS of BDS/GPS/GLONASS PPP float solutions are better than 1, 1 and 3 cm, respectively. The average values of the RMS are 0.7, 0.6 and 2.3 cm, respectively. The accuracy improved 68.2, 50.0, 50.0 % and 75.0, 68.4, 61.0 % than that of GPS-only and BDS-only PPP and improved 68.4, 61.0, 11.5 % than that of BDS/GPS PPP.

(2) Compared with float solutions, PPP fixed solutions improve greatly in the East, North and Up components. The average values of the RMS of BDS PPP fixed solutions are 1.6, 1.4 and 5.0 cm in East, North and Up components, respectively, which improve 42.9, 26.3 and 15.3 % than those of float ones. The average values of the RMS of GPS PPP fixed solutions are 1.2, 0.8 and 2.4 cm, respectively, which improve 45.5, 33.3 and 25.0 % than those of float ones. The average values of the RMS of BDS/GPS PPP fixed solutions are 0.7, 0.7 and 2.4 cm, respectively, which improve 43.8, 50.0, 52.0 % and 41.7, 12.5, 0.0 % than those of BDS-only and GPS-only fixed solutions, respectively. The RMS of BDS/GPS/GLONASS fixed solutions are 0.5, 0.5 and 2.1 cm, respectively, which improved 68.8, 64.3, 58.0 % and 58.3, 37.5, 12.5 % than those of BDS-only and GPS-only fixed solutions and improved 28.6, 28.6, 12.5 % than that of BDS/GPS fixed ones. They also improved 28.6, 16.7 and 8.7 % than those of BDS/GPS/GLONASS float ones;

(3) Combined BDS/GPS PPP float solutions can achieve the accuracy of GPS PPP fixed solutions. BDS/GPS/GLONASS PPP float solutions can achieve the accuracy of BDS/GPS fixed solutions and beyond the accuracy of the GPS fixed solutions.

Figures 2.7 and 2.8 show the time series of the differences of BDS-only, GPS-only, BDS/GPS and BDS/GPS/GLONASS PPP float solutions and fixed solutions against "ground truth" at WUHN and SXKL station. As we can see that:

(1) The differences of BDS PPP float and fixed solutions against "ground truth" are within ±2 cm in East and North components after convergence, which are very close to those of GPS PPP float and fixed solutions. The Up component of BDS PPP float and fixed solutions are within ±10 cm, which were worse than those of GPS. The North component of BDS PPP float solutions has the fastest convergence speed while the East component has the slowest speed. The reason may be that it takes a long time to make the ambiguity parameters converge. BDS PPP fixed solutions significantly reduce the convergence time. This is because phase observations were converted to precise distance measurement after ambiguities resolution. The parameters are estimated quickly and exactly which quickens the convergence speed.

(2) The East and North components of GPS PPP float and fixed solutions are within ±2 cm after convergence and the Up component is within ±5 cm.

(3) The East and North components of BDS/GPS PPP float and fixed solutions are within ±1 cm after the convergence and the Up component is within ±5 cm. The fusion of BDS/GPS PPP float solutions did not reduce the convergence

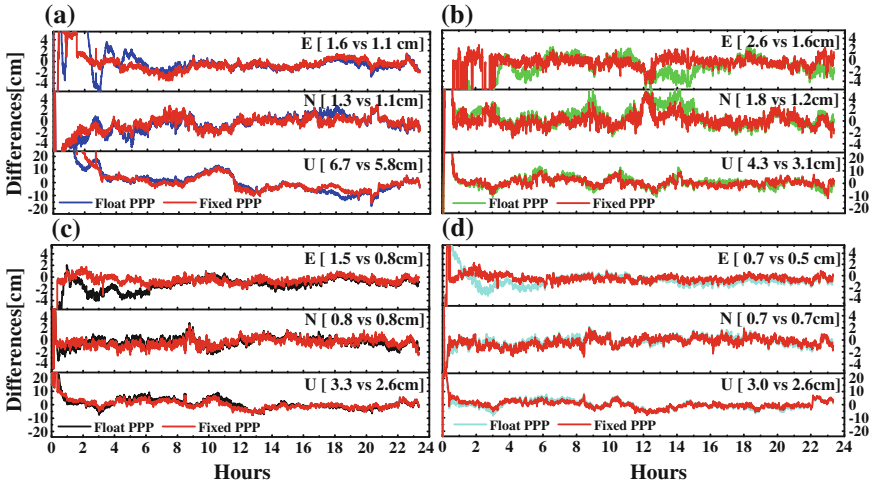

Fig. 2.7 Time series of float and fixed solutions of BDS-only, GPS, BDS/GPS and BDS/GPS/GLONASS PPP at WUHN. **a** BDS. **b** GPS. **c** BDS/GPS. **d** BDS/GPS/GLONASS

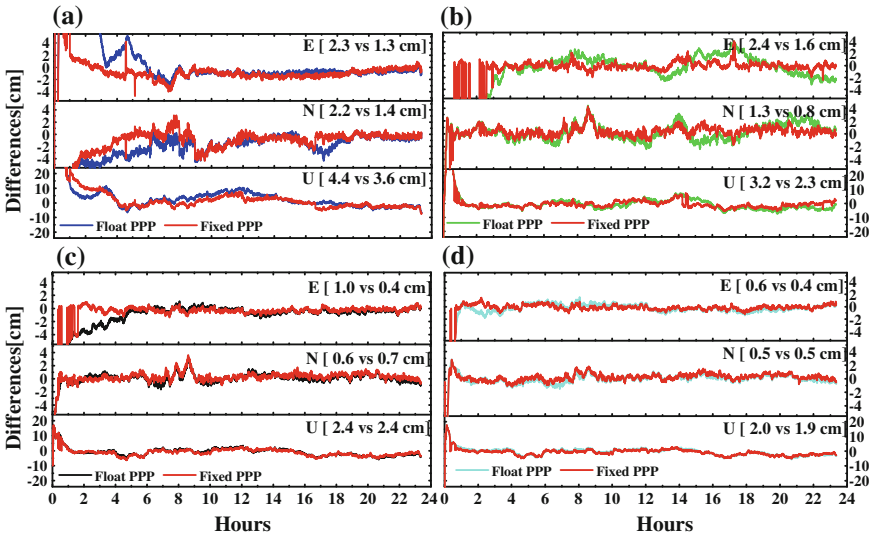

Fig. 2.8 Time series of float and fixed solutions of BDS-only, GPS-only, BDS/GPS and BDS/GPS/GLONASS PPP at SXKL. **a** BDS. **b** GPS. **c** BDS/GPS. **d** BDS/GPS/GLONASS

time significantly, which may due to the equal weighting of BDS and GPS observations.

(4) The East and North components of BDS/GPS/GLONASS PPP float and fixed solutions are within ±1 cm after the convergence and the Up component is within ±5 cm.

(5) The ambiguities resolution significantly accelerates the convergence speed and improves the positioning accuracy.

2.4.3 Systematic Bias Stability Analysis

Figure 2.9 shows the system time difference between BDS and GPS and between GLONASS and GPS at WUHN and SXKL station. We can see that the system time difference after convergence is relatively stable in the time domain. As Formulas 2.8 and 2.9 shown, the system time difference mainly depends on the pseudo-range hardware delay in the, which is quite stable in a day time.

2.4.4 Residual Analysis

Observation residuals contain measurement noise, multipath errors, orbit errors and dismodelled error such as receiver antenna PCV and PCO, which are important indicator of orbit determination and positioning accuracy [6]. Figure 2.10 shows the time series of BDS, GPS and GLONASS satellites LC and PC of all the 5 rovers.

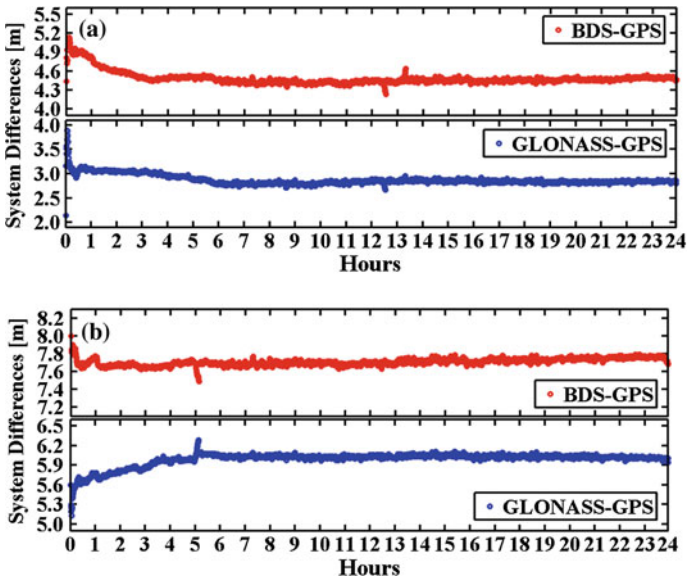

Fig. 2.9 Time series of system time difference between GLONASS and GPS and between BDS and GPS at WUHN and SXKL. **a** WUHN. **b** SXKL

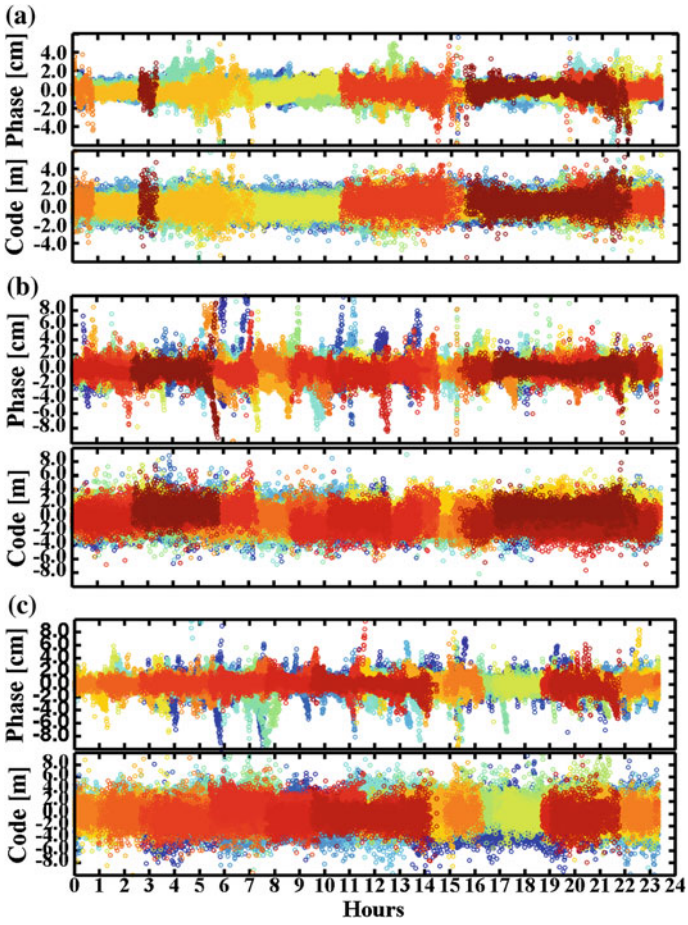

Fig. 2.10 Time series of BDS, GPS and GLONASS phase and code residuals of rovers. **a** BDS Residuals. **b** GPS Residuals. **c** GLONASS Residuals

Figure 2.11 shows the RMS of PC and LC of BDS, GPS and GLONASS satellites. It can be seen that the LC residuals of BDS, GPS and GLONASS are all within the ±2 cm. The PC residuals of BDS satellite are within ±2 m while those of GPS and GLONASS satellites are within ±4 m. The average values of BDS satellites LC and PC residuals RMS are 0.66 and 0.83 cm, respectively, which are less than those of GPS satellites LC and PC residuals RMS while GLONASS satellites have the largest LC and PC RMS values. The reason may be that all of the five rovers locate in China, where satellites observed are mainly IGSO and GEO in a day time, whose ambiguities are more stable compared to MEO satellites, which fit their observations better.

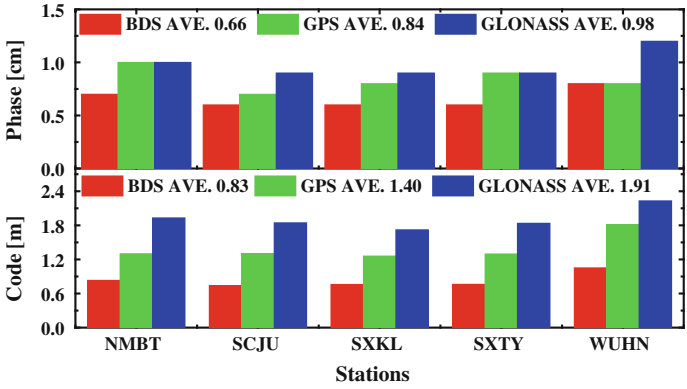

Fig. 2.11 RMS of BDS, GPS and GLONASS phase and code residuals of Rovers

2.5 Conclusions

In this article, we deduced the mathematical model of BDS/GNSS real-time kinematic PPP, studied the process and algorithm of un-differenced ambiguity resolution and realized the GNSS real-time kinematic PPP by fixing BDS-only, GPS-only and combined BDS/GPS ambiguities. Multi-GNSS data of reference stations from CMONOC were processed. We compared the accuracy of PPP float and fixed solution, studied the stability of wide-lane and narrow-lane FCB of BDS IGSO and MEO and GPS satellites, analyzed the stability of system time difference between BDS and GPS, GLONASS and GPS, respectively and compared the LC and PC residuals of BDS, GPS and GLONASS satellites. The following conclusions were acquired:

(1) The wide-lane FCB of BDS MEO satellites keep stable in time domain within 0.2 cycles while those of IGSO satellites are within 02–0.4 cycles. The narrow-lane FCB of BDS MEO and IGSO satellites keep stable within 0.2 cycles after convergence. The wide-lane and narrow-lane FCB of GPS satellites keep stable in time domain and the changes stay within 0.2 cycles;
(2) The fusion of multi-GNSS positioning raised the precision, reliability and continuity. The results of 5 rovers in this article showed that the precision were less than 1 cm in plane and 3 cm in vertical direction even without ambiguities resolution.
(3) The precision of GPS-only and BDS-only fixed solutions improved a lot than those of the real solutions. The precision raised 1–2 cm in three-dimension. Fixed the ambiguities of GPS and BDS at the same time improved further positioning performance. The convergence speed was accelerated after ambiguities especially for the east component.
(4) The system time differences between BDS and GPS and between GLONASS and GPS are very stable in the time domain.

We find that the fusion of multi-GNSS and the ambiguity resolution are the important ways to improve the accuracy of precise positioning and reduce the convergence time.

Acknowledgments We are grateful to the reviewers for their comments and suggestions. This work was supported by the "iGMAS" project of China, the National Nature Science Foundation of China (No. 41374034) and the National "863 Program" of China (Grant No. 2014AA123101).

References

1. China Satellite Navigation Office. BeiDou navigation satellite system signal In space interface control document open service signal B1I (version 1.0); 2012. http://www.beidou.gov.cn/attach/2012/12/27/201212275f2be9ad57af4cd09c634b08d7bc599e.pdf
2. Shi C, Zhao Q, Li M et al (2011) Precise orbit determination of Beidou satellites with precise positioning. China Sci Earth Sci 42(6):854–861
3. Shi C, Zhao Q, Hu Z, Liu J (2012) Precise relative positioning using real tracking data from COMPASS GEO and IGSO satellites. GPS Sol. doi: 10.1007/s10291-012-0264-x
4. Hauschild A, Montenbruck O, Sleewaegen J, Huisman L, Teunissen P (2012) Characterization of compass M-1 signals. GPS Sol. doi:10.1007/s10291-011-0210-3
5. Montenbruck O, Hauschild A, Steigenberger P, Hugentobler U, Teunissen P, Nakamura S (2012) Initial assessment of the COMPASS/BeiDou-2 regional navigation satellite system. GPS Sol. doi: 10.1007/s10291-012-0272-x
6. Zhao Q, Guo J, Li M, Qu L, Hu Z, Shi C, Liu J (2013) Initial results of precise orbit and clock determination for COMPASS navigation satellite system. J Geod. doi: 10.1007/s00190-013-0622-7
7. Yang Y, Li J, Xu J, Tang J, Guo H, He H (2011) Contribution of the compass satellite navigation system to global PNT users. Chin Sci Bull. doi: 10.1007/s11434-011-4627-4
8. Cai CS, Gao Y (2012) Modeling and assessment of combined GPS/GLONASS precise point positioning. GPS Sol. doi: 10.1007/s10291-012-0273-9
9. Li M, Qu L, Zhao Q, Guo J, Su X, Li X (2014) Precise point positioning with the BeiDou navigation satellite system. Sensors 14(1):927–943. doi:10.3390/s140100927
10. Qu L, Zhao Q, Li M, Guo J, Su X, Liu J (2013) Precise point positioning using combined BeiDou and GPS observations, vol 245, pp 241–252. doi:10.1007/978-3-642-37407-4_22
11. Zumberge JF, Heflin MB, Jefferson DC, Watkins MM, Webb FH (1997) Precise point positioning for the efficient and robust analysis of GPS data from large networks. J Geophys Res 102(B3):5005–5017
12. Ge M, Gendt G, Rothacher M, Shi C, Liu J (2008) Resolution of GPS carrier-phase ambiguities in precise point positioning (PPP) with daily observations. J Geod 82(7):389–399
13. Collins P, Bisnath S, Francois L, He´roux P (2010) Undifferenced GPS ambiguity resolution using the decoupled clock model and ambiguity datum fixing. Navigation 57(2):123–135
14. Laurichesse D, Mercier F, Berthias J, Bijac J (2008) Real time zero difference ambiguities blocking and absolute RTK. In: Proceedings of the ION NTM-2008, Institute of Navigation, San Diego, California, pp 747–755
15. Geng J, Teferle F, Shi C, Meng X, Dodson A, Liu J (2009) Ambiguity resolution in precise point positioning with hourly data. GPS Sol 13(4):263–270
16. Li XX, Zhang XH, Li P (2012) PPP for rapid precise positioning and orbit determination with zero-difference integer ambiguity fixing. Chin J Geophys 55(3):833–840 (in Chinese) doi: 10.6038/j. ISSN. 0001-5733.2012.03.013
17. Geng J, Meng X, Dodson A, Teferle F (2010) Integer ambiguity resolution in precise point positioning: method comparison. J Geod 84(9):569–581

18. Shi J, Gao Y (2013) A comparison of three PPP integer ambiguity resolution methods. GPS Solut 18(4):519–528. doi:10.1007/s10291-013-0348-2
19. Wanninger L (2011) Carrier-phase inter-frequency biases of GLONASS receivers. J Geod 86(2):139–148. doi:10.1007/s00190-011-0502-y
20. Dong DN, Bock Y (1989) Global positioning system network analysis with phase ambiguity resolution applied to crustal deformation studies in California. J Geophys Res Solid Earth 94(B4):3949–3966. doi:10.1029/JB094iB04p03949
21. Wu J, Wu S, Hajj G, Bertiger W, Lichten S (1993) Effects of antenna orientation on GPS carrier phase. Manuscr Geod 18:91–98
22. Zhao Q, Liu J, Ge M, Shi C (2006) Applications of square-root information filtering and smoothing on orbit determination of LEO satellites with on-board GPS data. Wuhan Univ J Geo Inf Sci 31:12–15

http://www.springer.com/978-3-662-46631-5

China Satellite Navigation Conference (CSNC) 2015
Proceedings: Volume III
Sun, J.; Liu, J.; Fan, S.; Lu, X. (Eds.)
2015, XX, 862 p. 430 illus., Hardcover
ISBN: 978-3-662-46631-5